Semiconductor Physics, Quantum Electronics & Optoelectronics, 2011. V. 14, N 4. P. 421-426.

PACS 72.20.-i, 72.80.Ey, 78.20.Ci

Energy band gap and electrical conductivity of $Cd_{1-x}Mn_xTe$ alloys with different manganese content

L.A. Kosyachenko[1], I.M. Rarenko[1], T. Aoki[2], V.M. Sklyarchuk[1], O.L. Maslyanchuk[1], N.S. Yurtsenyuk[1], Z.I. Zakharuk[1]

[1]*Yu. Fedkovych Chernivtsi National University, 2, Kotsyubinsky str., 58012 Chernivtsi, Ukraine*

[2]*Research Institute of Electronics, Shizuoka University, 3-5-1 Johoku, Hamamatsu 432-8011, Japan*

Abstract. The optical and electrical properties of single $Cd_{1-x}Mn_xTe$ (x = 0.07 - 0.40) crystals with *p*-type conduction and resistivity $10^4 - 10^8$ Ohm·cm have been studied. The band gaps of the samples and their temperature dependences have been determined. The electrical conductivity of this material and its temperature variation are explained in terms of statistics for electrons and holes in semiconductor with taking into account the compensation process. The energy of ionization and degree of compensation levels responsible for the electrical conductivity of the samples have been found.

Keywords: diluted semiconductors, $Cd_{1-x}Mn_xTe$, Mn content, band gap, compensated semiconductor.

Manuscript received 04.01.11; revised manuscript received 20.07.11; accepted for publication 14.09.11; published online 30.11.11.

1. Introduction

$Cd_{1-x}Mn_xTe$ is typical diluted magnetic semiconductor known to possess the zinc-blende structure within the range $0 < x < 0.77$. Owing to its unique magnetic and magneto-optic properties [1], $Cd_{1-x}Mn_xTe$ crystals can be used in many device applications, such as Faraday rotators, optical isolators, solar cells, magnetic field sensors and substrates for the epitaxial growth of $Hg_{1-x}Cd_xTe$ and $Hg_{1-x}Zn_xTe$ due to its chemical and structural compatibility [2]. More recently, $Cd_{1-x}Mn_xTe$ offers several potential advantages over $Cd_{1-x}Mn_xTe$ as a material for room-temperature X- and gamma-ray detectors [3, 4] that are widely used in science, medicine, industry, environment monitoring and other fields. Among them, $Cd_{1-x}Mn_xTe$ has a wide range of tunability of the band gap due to the large compositional influence of manganese. The band gap range 1.7 eV to 2.2 eV, required for substantiating an "ideal" radiation detector performance, can be realized with a relatively low (< 50%) amount of Mn compared with that of Zn in $Cd_{1-x}Mn_xTe$ (up to 70%) [44]. In fact, the energy band gap of $Cd_{1-x}Mn_xTe$ increases about 13 meV per atomic percent of Mn compared with 6.7 meV of Zn in $Cd_{1-x}Mn_xTe$. Another important advantage is that the segregation coefficient of Mn in CdTe is close approximately to unity as compared with 1.35 for Zn, that is, $Cd_{1-x}Mn_xTe$ crystals can have more homogenous distribution of Mn throughout the ingot. These notable characteristics of $Cd_{1-x}Mn_xTe$ increase the possibility of growing uniform large-volume stoichiometric crystals that can be potentially fabricated into different high-quality devices.

In this work, we study optical properties and mechanism of compensation of $Cd_{1-x}Mn_xTe$ single crystals with a different manganese content. The band gap and its temperature dependence are found from the optical transmission curves. Based on the experimental dependences of electrical characteristics inherent to this material and statistics of electrons and holes, we have succeeded in determining the ionization energy of the energy level responsible for the electrical conductivity and degree of its compensation. It seems that the obtained results lead to the conclusions which are important for technology.

2. Optical properties of $Cd_{1-x}Mn_xTe$ crystals

$Cd_{1-x}Mn_xTe$ *p*-type crystals have been grown by the modified melting method in graphite coated quartz

ampoules with continuous stirring alloy for better uniformity. The MnTe fraction for CdTe-MnTe was within the range $x = 0.07$ to 0.40.

As an example, Fig. 1 shows optical transmission spectra $T(\lambda)$ of a $Cd_{1-x}Mn_xTe$ wafer with the thickness 0.54 mm. As seen, in the $\lambda > 650 - 700$ nm range this material is quite transparent: at $\lambda = 1000$ nm the optical transmission equals 0.55 - 0.56.

According to the data from Ref. [6], the coefficient of reflection R for $Cd_{0.8}Mn_{0.2}Te$ at the wavelength 700 nm is 0.12 with trend of decreasing with increasing λ. The optical transmission of a wafer is determined by the expression where multiple reflections inside the sample are taken into account [7]:

$$T = \frac{(1-R)^2 \exp(-\alpha d)}{1 - R^2 \exp(-2\alpha d)}, \qquad (1)$$

where α is the absorption coefficient, d is the sample thickness.

In the region of transparency of the crystal, it is possible to ignore the absorption inside the crystal, i.e. at $\alpha = 0$ and $R = 0.12$ from Eq. (1) one obtains: $T = (1-R)/(1+R) = 0.79$. This value of T exceeds the $Cd_{1-x}Mn_xTe$ optical transmission at the wavelength 700 nm equal to 0.55 - 0.56 (Fig. 1). Therefore, we can assume that the transmission of the crystals under study within the range of transparency is substantially limited by impurities and defects, which, besides, reduce the lifetime of charge carriers and hence the detective properties of the material.

The performed studies of $T(\lambda)$ allowed us to obtain the absorption curve α in the region of interband transitions using the formula

$$\alpha = -\frac{1}{d}\ln\left\{\frac{1}{R^2}\left[-\frac{(1-R)^2}{2T} + \left[\frac{(1-R)^4}{4T^2} + R^2\right]^{1/2}\right]\right\}, \qquad (2)$$

which is a solution of Eq. (1).

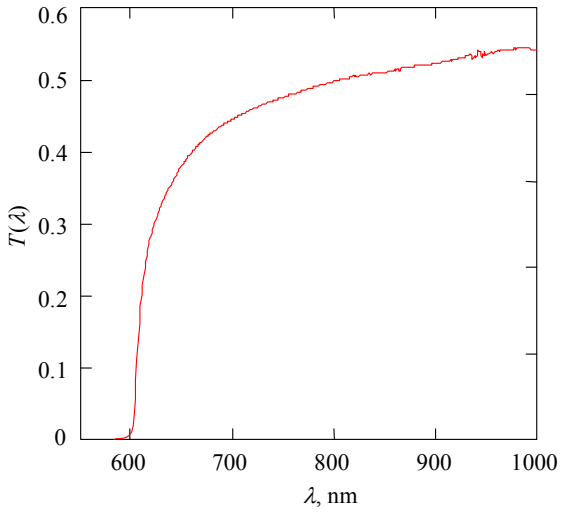

Fig. 1. Optical transmission spectra of $Cd_{1-x}Mn_xTe$ wafer at $T = 300$ K.

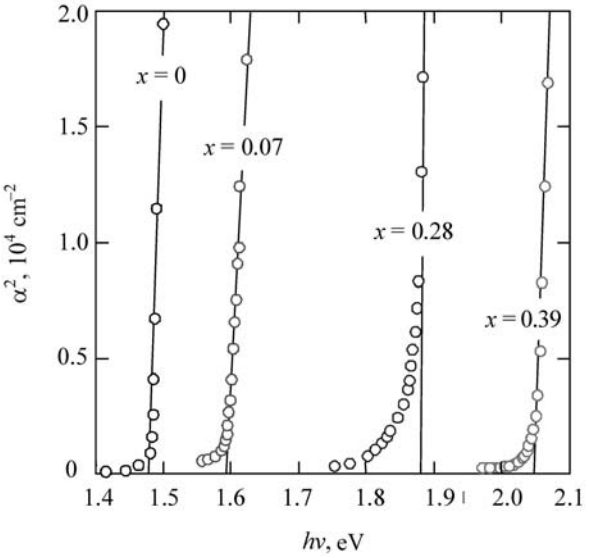

Fig. 2. Comparison of experimental absorption curves with Eq. (3) at $T = 300$ K for $Cd_{1-x}Mn_xTe$ crystals with different contents of Mn (parameter x) and for CdTe crystal.

Fig. 2 shows a comparison of the obtained absorption curves $\alpha(h\nu)$ ($h\nu$ is the photon energy) with the formula that describes the absorption edge for semiconductor with direct interband transitions such as $Cd_{1-x}Mn_xTe$ [7, 8]:

$$\alpha = \alpha_0(h\nu - E_g)^{1/2}, \qquad (3)$$

where α_0 is the coefficient that can be considered independently of $h\nu$ in the narrow spectral range $h\nu \approx E_g$.

To obtain a linear dependence in accord with Eq. (3), the curves $\alpha(h\nu)$ in Fig. 2 are plotted in coordinates α^2 vs $h\nu$. Fig. 2 shows that the dependence $\alpha(h\nu)$ in the range of large α is consistent with Eq. (3), which justifies the $Cd_{1-x}Mn_xTe$ as semiconductor with direct interband transitions (Table 1). Extrapolation of linear plots of α^2 vs $h\nu$ (at the edge of transmission $h\nu \approx E_g$) to the intersection with the abscissa axis allows us to determine accurately the band gap of the investigated crystals.

The dependences of E_g on x for $Cd_{1-x}Mn_xTe$ crystals were investigated in several works [9 – 12]. The graphical comparison shows that the dependence E_g on x for $Cd_{1-x}Mn_xTe$ obtained by various authors are quite close within the range $x = 0.2 - 0.5$ but appreciably different at $x = 0$ (i.e. for CdTe) within 1.47 – 1.53 eV [11]. Our detailed measurements of optical transmission spectra carried out on pure and perfect single crystals of Acrorad Corporation show that the CdTe band gap at 270 – 300 K is 1.47 – 1.48 eV. Therefore, for determining the content of Mn in the $Cd_{1-x}Mn_xTe$ single crystals we used the dependence $E_g(x)$ from [10], which gives the best agreement with our E_g value for CdTe:

$$E_g = 1.47 + 1.45\,x. \qquad (4)$$

Table 1. The parameters of $Cd_{1-x}Mn_xTe$ single crystals under study obtained from optical measurements.

Material	x	E_g (300 K), eV	ρ at 300 K, Ohm·cm	E_g (0 K), eV	$-dE_g/dT$ (10^{-4} eV/K)
CdTe	0	1.476	$4\cdot10^9$	1.605	4.3
$Cd_{1-x}Mn_xTe$	0.072	1.59	$2.48\cdot10^4$	1.723	4.42
$Cd_{1-x}Mn_xTe$	0.277	1.875	$1.5\cdot10^8$	2.0495	5.7
$Cd_{1-x}Mn_xTe$	0.399	2.045	$7.13\cdot10^7$	2.244	6.72

Table 2. The electrical parameters of $Cd_{1-x}Mn_xTe$ single crystals under study at 300 K.

Material	ρ, Ohm·cm	ρ_i, Ohm·cm	E_g, eV	ΔE, eV	E_a, eV	Δμ, eV	$\xi=N_d/N_a$
CdTe	$4\cdot10^9$	$6\cdot10^9$	1.476	0.80	0.82	0.69	0.006
$Cd_{0.93}Mn_{0.07}Te$	$2.48\cdot10^4$	$2.1\cdot10^{10}$	1.59	0.3	0.3	0.33	0.98
$Cd_{0.72}Mn_{0.28}Te$	$1.5\cdot10^8$	$7.82\cdot10^{13}$	1.875	0.5	0.41	0.63	0.9997
$Cd_{0.6}Mn_{0.4}Te$	$7.13\cdot10^7$	$1.28\cdot10^{15}$	2.045	0.5	0.41	0.61	0.9995

Hence, from the found value of band gap at 300 K we can determine the Mn content in the investigated crystals by using Eq. (4) as $x = (E_g - 1.47)/1.45$. The data obtained in this way are listed in Table 1.

From a practical point of view, the important characteristic required among other things to calculate the conductivity is the temperature dependence of the semiconductor band gap $E_g(T)$. Fig. 3 shows the absorption curves for the $Cd_{0.93}Mn_{0.07}Te$ crystal obtained at various temperatures. Fig. 4 presents the temperature dependence of the band gap found from the intersection of straight section of plots with the abscissa axis similar to those in Fig. 3 for crystals with various contents of Mn.

As seen from Fig. 4, the $E_g(T)$ temperature dependences can be described by linear functions that can be represented as

$$E_g(T) = E_g(0) - \gamma T, \qquad (4)$$

where $E_g(0)$ is the band gap at $T \to 0$, and γ is its temperature coefficient.

As seen from comparison of the data shown in Fig. 5, the dependence of the energy gap temperature coefficient on the Mn content in $Cd_{1-x}Mn_xTe$ is in good agreement with the results given in Ref. [9].

3. Electrical properties of $Cd_{1-x}Mn_xTe$ single crystals

For electrical measurements, ohmic contacts to $Cd_{1-x}Mn_xTe$ crystals were made by vacuum evaporation of nickel. Prior the deposition, crystal surface was chemically treated. As seen from Fig. 6, the contacts provide linearity of current-voltage characteristics in a wide voltage range. This is the case for both polarities of the applied voltage.

Fig. 7 represents the temperature dependences of the resistivity ρ of $Cd_{1-x}Mn_xTe$ crystals with different Mn content, as well as for high-resistance CdTe for comparison. As seen, the temperature dependences of all samples in the coordinates lg(ρ) vs $1000/T$ agree with the expected linear functions. The room-temperature resistivity of $Cd_{0.93}Mn_{0.07}Te$ ($E_g = 1.59$ eV) is $2.48\cdot10^4$ Ohm·cm, for $Cd_{0.72}Mn_{0.28}Te$ ($E_g = 1.875$ eV) is much higher and equal to $1.5\cdot10^8$ Ohm·cm, but for sample with wider band gap $Cd_{0.60}Mn_{0.40}Te$ ($E_g = 2.045$ eV) is not higher but even a somewhat lower. The observed values of ρ for all $Cd_{1-x}Mn_xTe$ crystals are much lower than the resistivity of samples of these materials with intrinsic conductivity

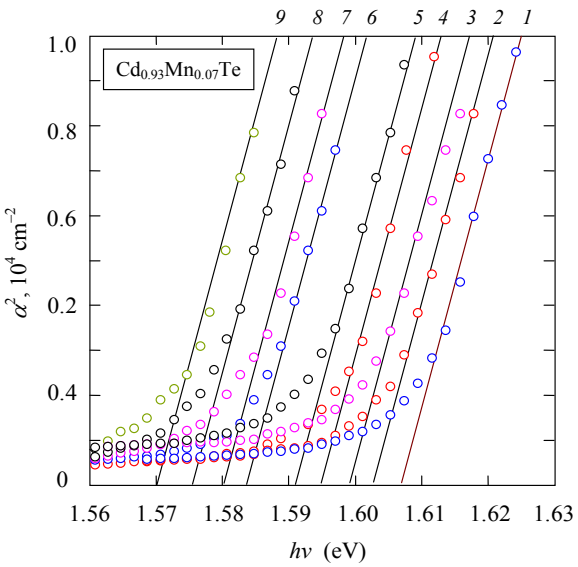

Fig. 3. Dependences of the absorption coefficient α on the photon energy $h\nu$ in a narrow range near $h\nu \approx E_g$ obtained from the transmission curves of $Cd_{0.93}Mn_{0.07}Te$ at temperatures: *1* – 268, *2* – 275, *3* – 281, *4* – 293, *5* – 299, *6* – 310, *7* – 322, *8* – 333, *9* – 344 K (circles – experimental results, lines – linear approximations of dependences α^2 vs $h\nu$).

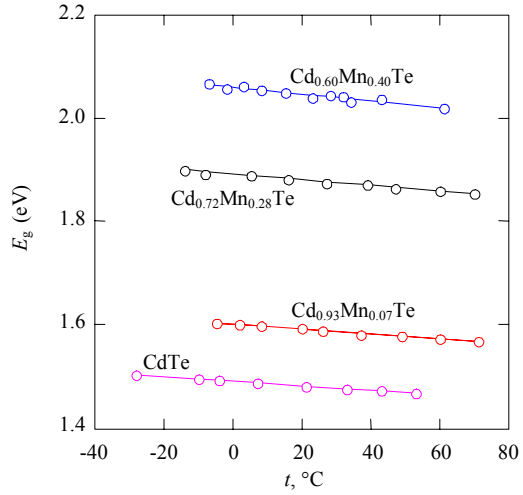

Fig. 4. Temperature dependences of the band gap of $Cd_{1-x}Mn_xTe$ ($x = 0$ - 0.40).

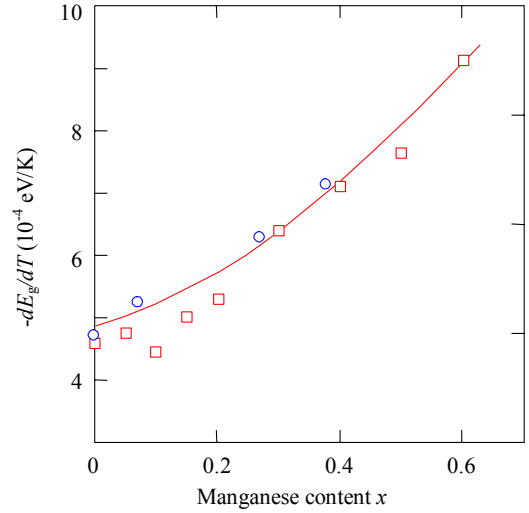

Fig. 5. The dependence of the temperature coefficient of band gap on the Mn content in $Cd_{1-x}Mn_xTe$ (circles are the results of our experiments, boxes are the results taken from [9]).

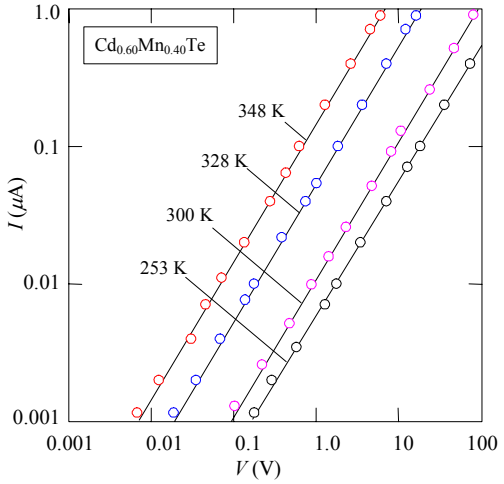

Fig. 6. The current-voltage characteristics of $Cd_{0.60}Mn_{0.40}Te$ single crystal with ohmic contacts at different temperatures.

$$\rho_i = \frac{1}{qn_i\mu_n + qn_i\mu_p}, \qquad (5)$$

where q is the elementary charge, μ_n and μ_p are the mobilities of electrons and holes, respectively, n_i is the intrinsic carrier concentration

$$n_i = \sqrt{N_c N_v}\,\exp\left(-\frac{E_g}{2kT}\right), \qquad (6)$$

where $N_c = 2(m_n^* kT/2\pi\hbar^2)^{3/2}$ and $N_v = 2(m_p^* kT/2\pi\hbar^2)^{3/2}$ are the effective densities of states in the conduction and valence bands, respectively.

Data on the effective masses of electrons m_n^* and holes m_p^* in $Cd_{1-x}Mn_xTe$ with different Mn content is not mentioned in literature, therefore to estimate them we take their values the same as for CdTe, i.e. $m_n^* = 0.11m_0$, $m_p^* = 0.35m_0$ (m_0 is the electron mass in vacuum). Substituting the found value of E_g in Eq. (6), and, again, for an estimation we take $\mu_n = 1000$ cm^2/(V·s) and $\mu_p = 100$ cm^2/(V·s) in Eq. (5) for the resistivities. For $Cd_{0.93}Mn_{0.07}Te$, $Cd_{0.72}Mn_{0.28}Te$ and $Cd_{0.60}Mn_{0.40}Te$ with intrinsic conductivities at 300 K one obtains: $\rho_i = 2.1\cdot10^{10}$, $7.82\cdot10^{13}$ and $1.28\cdot10^{15}$ Ohm·cm, respectively. The found from Eq. (5) values exceed the resistivity of the investigated crystals and CdTe with almost its intrinsic conductivity. We believe this is due to the extrinsic (impurity) character of electrical conduction of $Cd_{1-x}Mn_xTe$ crystals.

As known, even high-purity CdTe crystals and, most probably, $Cd_{1-x}Mn_xTe$ crystals commonly contain high concentrations of residual impurities and intrinsic defects of both the donor and acceptor types. Therefore, explaining the above electrical characteristics it is naturally to apply the compensated semiconductor model. Bearing in mind the hole type of conductivity for this material, we can accept the Fermi level and electrical conductivity of the material to be determined by acceptor with the ionization energy E_a and the concentration N_a. Denoting the concentration of compensating donors by N_d, for the electroneutrality equation for this semiconductor one can write:

$$n + N_a^- = p + N_d^+, \qquad (7)$$

where N_a^- and N_d^+ are the concentrations of charged donors and acceptors, respectively.

For wide-band semiconductor under discussion, the Fermi level is located far from the top of valence band and the impurity (defect) concentrations are significant. Therefore, we can neglect the concentrations of free carriers n and p in Eq. (7). If the level of compensating donors is shallow enough, they can be considered as fully ionized, i.e. we can accept $N_d^+ \approx N_d$. With these simplifications Eq. (7) reduces to the expression:

$$\frac{N_a}{\exp\left(\dfrac{E_a-\Delta\mu}{kT}\right)+1}=N_d\,. \qquad (8)$$

The analytical solution of Eq. (8) has the form

$$\Delta\mu = E_a - kT\ln\left(\frac{1-\xi}{\xi}\right), \qquad (9)$$

where Δμ is the energy of the Fermi level measured from the top of the valence band, $\xi = N_d/N_a$ is the degree of compensation of acceptors by donors.

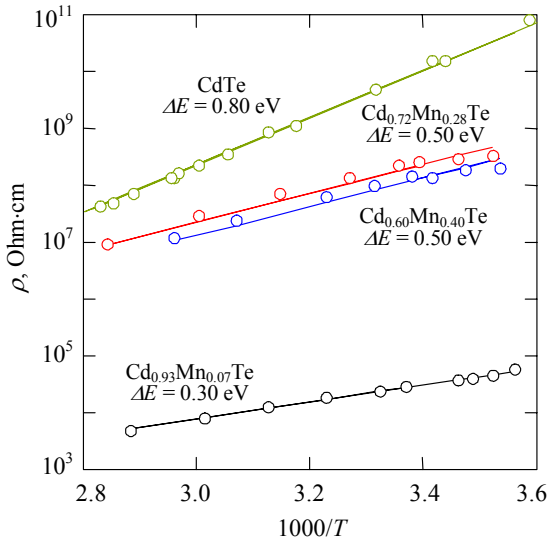

Fig. 7. Temperature dependences of resistivity ρ of $Cd_{1-x}Mn_xTe$ single crystals (x = 0.07, 0.27, 0.40) as well as high-resistance CdTe for comparison. The activation energies of the conductivity ΔE are also shown.

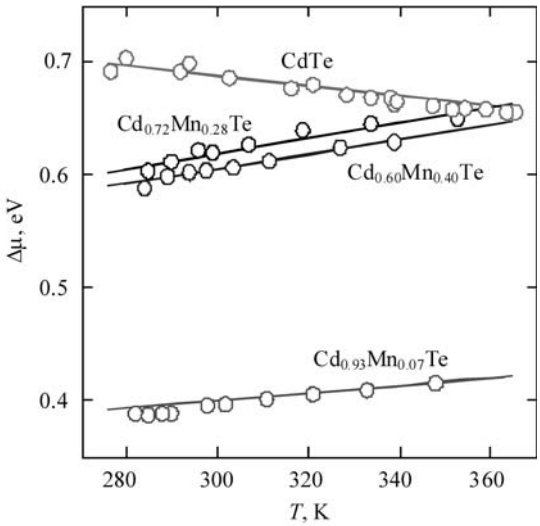

Fig. 8. The temperature dependence of the Fermi level energy Δμ (measured from the top of the valence band) calculated by Eq. (9) (solid lines) and obtained from the curves presented in Fig. 7 using Eq. (10) (circles).

Fig. 8 shows the temperature dependence of Δμ found from experimental dependencies ρ(T) in Fig. 7 as

$$\Delta\mu = kT\ln\left(\frac{N_v}{p}\right), \qquad (10)$$

where $p = 1/q\rho\mu_p$. In the calculations, we ignore the weak temperature dependence of hole mobility $\mu_p(T)$ and effective densities of states in the valence bands $N_v(T)$, because the narrow range of temperatures 280 – 360 K compared with the ρ(T).

As one can see from Fig. 8, the Fermi level is shifted markedly in the band gap at temperature variations, and there are qualitative differences in behavior of Δμ(T) for different samples. For the $Cd_{1-x}Mn_xTe$ crystals, the energies of the Fermi level Δμ increase with temperature, whereas for semi-insulating CdTe, Δμ decreases with temperature. Our analysis shows that the difference between the resistivity of materials determined experimentally and calculated for intrinsic semiconductors is associated with a different degree of compensation in these materials. Comparison of the experimental dependence Δμ(T) found from Eq. (10) with the theoretical curves calculated using Eq. (9) confirms this suggestion.

Comparison of calculated and experimental dependences Δμ(T) allows us to determine with a rather high accuracy the ionization energy E_a of the level responsible for the electrical conductivity of each sample and the degree of compensation ξ of acceptors by donors. Note that the experimental data coincide with the results of calculation only for one combination of E_a and ξ. Variation of E_a leads to a shift along the vertical axis, and variation of ξ leads to change of the angle of dependence Δμ(T). The values of E_a and ξ obtained from such manipulations, as well as other parameters of $Cd_{1-x}Mn_xTe$ and CdTe single crystals are summarized in Table 2. A high compensation degree ξ of local levels (0.98 - 0.9997), which is typical for the effect of self-compensation impurity centers, attracts attention. It is similar to the observed values of ξ in CdTe, $Cd_{1-x}Zn_xTe$, CdS and other semiconductors [13 – 16].

4. Conclusions

The optical and electrical properties of $Cd_{1-x}Mn_xTe$ crystals with a resistivity of $10^4 - 10^8$ Ohm·cm in the wide range of Mn content x = 0.07 – 0.40 have been studied. The band gaps of the samples 1.59 – 2.045 eV at 300 K and their temperature coefficient $(4.4 - 6.7) \times 10^{-4}$ eV/K have been determined. It has been shown that the conductivity of materials is determined by impurities (defects), which create energy levels in the band gap, rather than by the width of the band gap. The ionization energies of these impurities (defects) 0.3 - 0.41 eV and degree of compensation 0.98 - 0.9997 for the levels responsible for the electrical conductivity of the samples under study have been found.

References

1. J.K. Furdyna, Diluted magnetic semiconductors // *J. Appl. Phys.* **64**(4), p. R29-R64 (1988).
2. R. Triboulet, A. Heurtel, and J. Rioux, Twin-free (Cd, Mn)Te substrates // *J. Cryst. Growth,* **101**, p. 131 (1990).
3. A. Burger, K. Chattopadhyay, H. Chen, J.-O. Ndap, X. Ma, S. Trivedi, S.-W. Kutcher, R. Chen, R.-D. Rosemeier, Crystal growth, fabrication and evaluation of cadmium manganese telluride gamma ray detectors // *J. Cryst. Growth*, **198/199**, p. 872-876 (1999).
4. J.E. Toney, T.E. Schlesinger, R.B. James, Optimal bandgap variants of $Cd_{1-x}Zn_xTe$ for high-resolution X-ray and gamma-ray spectroscopy // *Nucl. Instr. and Meth. A,* **428**(1), p. 14 (1999).
5. A. Mycielski, A. Burger, M. Sowinska, M. Groza, A. Szadkowski, P. Wojnar, B. Witkowska, W. Kaliszek, and P. Siffert, Is the (Cd,Mn)Te crystal a prospective material for X-ray and γ-ray detectors? // *Phys. Status Solidi* (*c*), **2**, p. 1578 (2005).
6. L. Safonova, R. Brazis, R. Narkowicz, Optical properties of CdMnTe crystals near fundamental absorption edge in transverse magnetic fields // *J. Alloys and Compounds*, **371** (1-2), p. 177-179 (2004).
7. J.I. Pankove, *Optical Processes in Semiconductors*, New Jersey, Prentice-Hall, 1973.
8. S. Adachi, *Optical Properties of Crystalline and Amorphous Semiconductors: Materials and Fundamental Principles.* Kluwer, Academic Publishers Dordrecht, 1999.
9. N. Bottka, J. Stankiewicz, W. Giriat, Electroleflectance studies in $Cd_{1-x}Mn_xTe$ solid solutions // *J. Appl. Phys.* **52**(6), p. 41-89 (1981).
10. M. El Amrani, J.P. Lascaray, J. Diouri, Fundamental absorption of $Cd_{1-x}Mn_xTe$ crystals // *Solid State Communs.* **45**, p. 351-353 (1983).
11. L.A. Kosyachenko, I.M. Rarenko, V.M. Sklyarchuk, N.S. Yurtsenyuk, O.L. Maslyanchuk, O.F. Sklyarchuk, Z.I. Zakharuk, E.V. Grushko, $Cd_{1-x}Mn_xTe$ as a material for X- and γ-ray detectors // *Sensor Electronics and Microsystem Technology* **1**(**7**), p. 74-80 (2010).
12. R. Bucker, H.-E. Gumlich, M. Krause, The influence of the temperature and the composition on reflectivity of $Cd_{1-x}Mn_xTe$ within the spectral range $1.5 \le E \le 4$ eV // *J. Phys. C: Solid State Phys.* **18**, p. 661-667 (1985).
13. G. Mandel, Self-compensation limited conductivity in binary semiconductors // *Phys. Rev. A,* **134**, p. 1073-1079 (1964).
14. F.F. Morehead and G. Mandel, Self-compensation limited conductivity in binary semiconductors. IV. $n-Zn_xCd_{1-x}Te$ // *Phys. Rev. A,* **137**, p. 924-925 (1965).
15. U.V. Desnica, I.D. Desnica-Frankovic, R. Magerle, A. Burchard, M. Deicher, Experimental evidence of the self-compensation mechanism in CdS // *J. Cryst. Growth,* **197**, p. 612-615 (1999).
16. S. Lany, H. Wolf and Th. Wichert, DX-centers in CdTe and ZnTe observed by locally sensitive probe atoms // *Mat. Res. Soc. Symp. Proc.* **763**, p. B1.3.1-B1.3.6 (2003).